Journal of Power Sources 245 (2014) 520–528

Contents lists available at SciVerse ScienceDirect

Journal of Power Sources

journal homepage: www.elsevier.com/locate/jpowsour

Stainless steel fiber felt as cathode diffusion backing and current collector for a micro direct methanol fuel cell with low methanol crossover

Yang Li [a], Xuelin Zhang [a,b,*], Li Nie [a], Yufeng Zhang [a], Xiaowei Liu [a]

[a] MEMS Center, School of Astronautics, Harbin Institute of Technology, Harbin 150001, China
[b] National Key Laboratory of Fundamental Science of Micro/Nano-Device and System Technology, Chongqing University, Chongqing 400044, China

HIGHLIGHTS

- Stainless steel fiber felt was used as cathode current collector and backing layer.
- Methanol crossover was lowered obviously.
- Higher fuel utilization ratio and energy efficiency were achieved.

ARTICLE INFO

Article history:
Received 8 April 2013
Received in revised form
20 June 2013
Accepted 20 June 2013
Available online 28 June 2013

Keywords:
Direct methanol fuel cell
Membrane electrode assembly
Methanol crossover
Stainless steel fiber felt
Current collector

ABSTRACT

In this paper, a membrane electrode assembly (MEA) with novel structure is designed and fabricated for a micro direct methanol fuel cell (DMFC), which used stainless steel fiber felt (SSFF) to replace the current collector and the backing layer at cathode. Result data shows that the novel structure can reduce the methanol crossover dramatically, as a result, achieves a better performance with a higher methanol concentration, a higher fuel utilization ratio and energy efficiency. In addition, the novel MEA also presents an improved water management at room temperature, allowing it to achieve a better performance. To elaborate the effect of the novel structure on anode or cathode electrode process, a reference electrode is built inside the single cell. The electrochemical results of half-cell test show that the novel MEA has a greatly reduced cathode polarization and a slightly increased anode polarization.

1. Introduction

Direct methanol fuel cell (DMFC) is an attractive and a leading candidate power source for portable and micro-power devices due to its simple structure, high specific energy, and instantaneous recharging time [1,2]. In order to make the DMFC more competitive with conventional battery technologies, it would be optimal to operate the DMFC in a passive mode, which has no auxiliary liquid pump and gas blower compressor but relies on diffusion and natural convection to supply the fuel and oxygen.[3]. Although the passive design greatly simplify the cell structure, the power density from passive systems is not as good as those running in an active mode due to poor transport. To achieve the commercialization of a passive DMFC, various passive DMFCs have been proposed and extensively investigated to improve the cell performance over the past decade [3].

Methanol crossover is one of the main challenges that restrain the performance of a passive DMFC [4,5]. The oxidation of methanol transporting from anode to cathode leads to a mixed potential and thus reduces the overall cell voltage. This problem can be solved by developing an alternative proton exchange membrane with high proton conductivity and low methanol permeability or modifying Nafion membrane to lower its methanol crossover [6–8]. Another way to lower methanol crossover is to optimize the MEA structure, the material of the gas diffusion layer (GDL) and even the structure of the current collector and reservoirs. By increasing the methanol transportation resistance from reservoirs to anode catalyst layer or adopting a pervaporation membrane, a passive DMFC can be operated at high methanol concentration or neat methanol with a low methanol crossover [9–13]. Moreover, methanol crossover can

* Corresponding author. MEMS Center, School of Astronautics, Harbin Institute of Technology, Harbin 150001, China. Tel.: +86 0451 86413442; fax: +86 0451 86413441.
E-mail address: zhangxuelin@hit.edu.cn (X. Zhang).

0378-7753/$ – see front matter © 2013 Elsevier B.V. All rights reserved.
http://dx.doi.org/10.1016/j.jpowsour.2013.06.122

also be reduced by enhancing water back diffusion from cathode to anode, which can be achieved by increasing the liquid pressure inside the cathode catalyst layer [14–18]. However, there are few researches that can reduce methanol crossover dramatically by optimizing the MEA structure.

In recent years, metallic porous materials, such as stainless steel fiber felt (SSFF), metal foam, have shown great potential to replace conventional carbon-based fiber products as backing layer of gas diffusion electrode due to high mechanical strength and good ductility. It was shown that SSFF GDL has larger compressive modulus, tensile modulus and ductility which is of great benefit to the transport ability under assembly compression and durability under the running conditions of shock and vibration [19]. By adopting SSFF as anode gas diffusion backing, an air-breathing DMFC gives better performance than that uses common carbon paper [20]. Because of its high electronic conductivity, porous metal foam can be used as both gas diffusion backing and current collector, which not only simplifies the cell structure but also gives better oxygen transportation than conventional gas diffusion layer [21]. But there is not a detailed study about how the electrode process is affected by this novel structure of membrane electrode assembly.

In this paper, a 316L stainless steel fiber felt was used as cathode gas diffusion backing and current collector to fabricate a MEA for DMFC. To evaluate effects of this novel MEA structure on cathode or anode electrode process, a half-cell measurement system was built by introducing an Ag/AgCl reference electrode. The fabricated micro DMFC was tested by polarization at different methanol concentrations, temperatures, constant-current discharging and electrochemical impedance spectra (EIS) tests in half-cell measurement system, comparing with a normal DMFC as reference.

2. Experiment

2.1. Fabrication of membrane electrode assembly

The membrane electrode assembly with an active area of 1 cm [2] was fabricated in-house by the following procedures. A stainless steel fiber felt made of 316L was coated with a 200 nm Au layer by magnetic sputtering technology to decrease the contact resistance. A mixture of 90 wt.% XC-72 and 10 wt.% PTFE was sprayed onto the surface of SSFF, serving as micro porous layer with a carbon loading of 4 mg cm^{-2}. Carbon-supported catalyst, 40 wt.% Pt/C, purchased from Johnson Matthey, Inc., was used for the fabrication of cathode catalyst layer. Catalyst ink was prepared by dispersing appropriate amount of catalyst and Nafion solution (Dupont, 5 wt.%) into a mixture of isopropyl alcohol and deionized (DI) water with a volume ratio of 1:1, and it was then sprayed onto the carbon-coated SSFF to get a cathode gas diffusion electrode (GDE). The Pt loading was about 2 mg cm^{-2} with 20 wt.% Nafion as the bonding agent. Along with the manufacture of the novel cathode GDE, a conventional cathode GDE with carbon paper (TGPH060) as backing layer was also made for reference. Some parameters of stainless steel fiber felt (SSFF) and carbon paper (CP) are presented in Table 1. Nafion 117 membrane was used to fabricate the MEA, which was pretreated in deionized water, 3 wt.% H_2O_2, 3 wt.% H_2SO_4, and deionized water again for 1 h in each solution in turn. Commercial anode gas diffusion electrode (purchased from Johnson Matthey, Inc.) and home-made cathode gas diffusion electrode were attached to Nafion membrane by hot-pressing at 408 K and 18 MPa for 180 s to form a MEA. Fig. 1(a) shows the prepared novel MEA. In following the two MEAs fabricated with carbon paper and SSFF were named respectively as CP-MEA and SSFF-MEA for the simplicity of description.

Table 1
Physical property of carbon paper and stainless steel fiber felt.

	Material density (g cm^{-3})	Bulk density (g cm^{-3})	Thickness (mm)	Porosity (%)	Fiber diameter (μm)
SSFF	7.98	2.73	0.36	65.8	10
Carbon paper	1.80	0.49	0.17	73	8

2.2. Single cell assembly

SSFF-MEA has SSFF as cathode current collector, and thus only an anode current collector is needed for single cell assembly, which has parallel channels with an open ratio of 43.2% [22]. For CP-MEA, a cathode current collector is still needed, which has perforated flow field with an open ratio of 40.7% [22]. All the current collector plates were made of 0.45 mm thickness 316L stainless steel, with 200 nm Au layer to reduce the contact resistance. The entire cell was assembled by holding the MEA and current collectors together between two organic glass fixtures. There is no external pump used in our passive DMFC system. Air is only supplied to the electrodes by diffusion through the open areas. A 2.5 mL reservoir is adhered to the anode fixture. Referring to the study of S. H. Yang, [23] an improved half-cell test system was set up. In this system, an Ag/

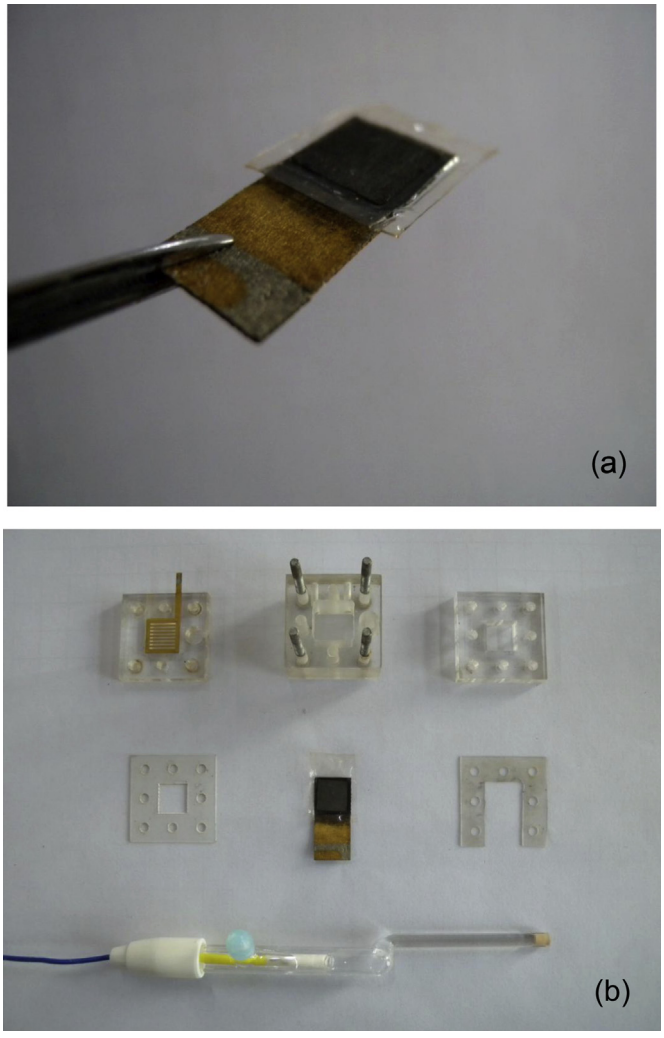

Fig. 1. Photographs of SSFF-MEA (a) and all parts of the single cell (b).

AgCl electrode was inserted into the cell through openings in the organic glass fixtures to contact the region of constant potential (RCP; 1.5 times the membrane thickness beyond the electrode edge) [24–26]. What's different from the configurations invented by S. H. Yang is that, to ensure a continuous electrolyte path between the reference electrode and the membrane surface, a 0.6 wt.% H_2SO_4 liquid column was sealed between the top of the Ag/AgCl electrode and the membrane, which will also reduce the chloride ion leakage from the Ag/AgCl electrode. In this system, the electrochemical measurement of anode or cathode electrode process can be carried out separately. Fig. 1(b) shows all the apartments of the single cell including the Ag/AgCl electrode.

2.3. Operating conditions and electrochemical measurement

Prior to the performance test, the cell was activated with 2 M methanol solution at 298 K [27]. And then, current–voltage (i–V) and current–power (i–P) curves were obtained at different conditions by gradually increasing the current at the rate of 10 mA. The current holding time per one step was 120 s. In addition, the cathode current–electrode potential (i–E) curves were measured for the cathode electrode process of the single cell. In-situ EIS measurement of the operating cell was performed in the frequency range from 10^6 Hz to 10^{-3} Hz with amplitude of ±10 mV. For measurement of the half-cell impedance of the anode (or cathode), the cathode (or anode) electrode was operated as a counter electrode. All the electrochemical measurements were conducted by CHI 604C electrochemical instrument (Shanghai, China).

3. Results and discussion

3.1. Characterization of stainless steel fiber felt

Before MEA performance test, the physical properties of stainless steel fiber felt were studied firstly. The surface morphology of SSFF was examined by scanning electron microscopy and shown in Fig. 2. It reveals that SSFF is made from stainless steel fiber of 9–11 μm in diameter with uniform porous inner configuration, which makes SSFF an eligible substitute for the diffusion backing of MEA.

Since SSFF serves as cathode backing layer and current collector, its wettability has great influences on the water and gas managements. The wettability test can be carried out by measuring the contact angle at which a liquid/vapor interface meets the solid surface, and a smaller contact angle usually means a more hydrophilic surface [28]. As shown in Fig. 3, water contact angles of different surfaces were examined immediately after dropping of deionized water (5 μl). It can be seen that SSFF has a contact angle of 112°, smaller than that of carbon paper (121°). It seems that the test result of SSFF in Fig. 3(a) is not in agreement with that describes in Ref. [29]. This contradiction should arise from the difference in diameter of single stainless steel fiber, porosity and thickness of SSFF, which can influence the wettability of SSFF significantly. Actually, copper is a more wettability material than stainless steel or aluminum [30], but its sintered fiber felt with 4 mm in thickness can have a contact angle of 136° [31]. Therefore, it is quite acceptable that SSFF can have a contact angle of 112°.

In the following sections, the cells fabricated with SSFF-MEA and CP-MEA were tested and compared, and when discussing the performance, the phrase of SSFF-MEA or CP-MEA usually means the cell fabricated with the corresponding MEA. Because the mechanical strength of 0.39 mm thickness SSFF is high enough to provide the MEA with the required assembly pressure, which makes it not necessary to adopt another current collector for a SSFF-MEA when fabricating a cell. CP-MEA has carbon paper as backing layer. Because carbon paper is very fragile and cannot provide the

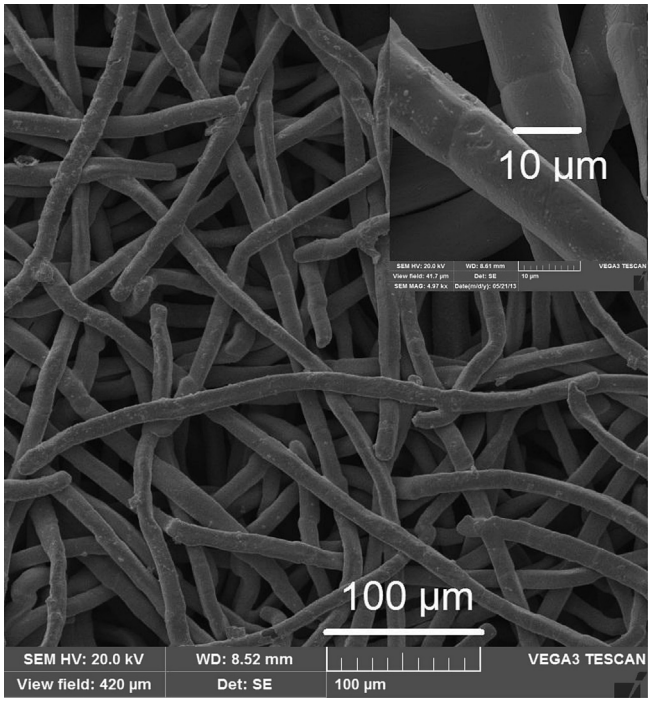

Fig. 2. Scanning electron microscopy image of SSFF.

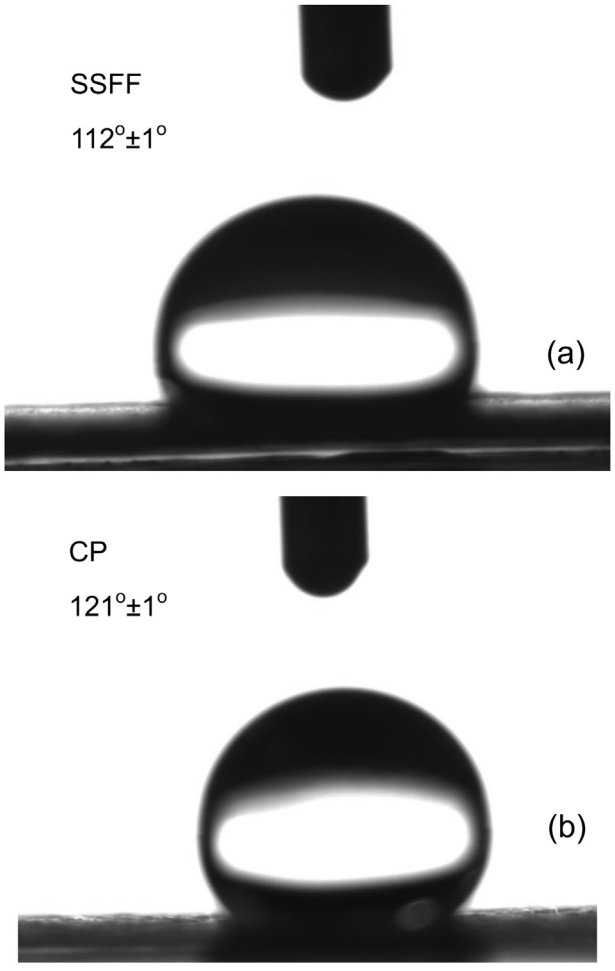

Fig. 3. Contact angles of the stainless steel fiber felt (a) and the carbon paper (b).

required mechanical strength, it is quite necessary to adopt a cathode current collector with high mechanical strength to maintain the good interfacial contact when fabricating a cell. Therefore, it is an inevitable case that the two MEAs were tested in different cathode configurations.

3.2. Performance tests at different methanol concentrations

Methanol concentration has significant effects on the MEA performance. High methanol concentration can decrease anode polarization by enhancing methanol transportation, but it can also accelerate methanol crossover, leading to deterioration of the cathode performance. Fig. 4 shows the power density curves of SSFF-MEA and CP-MEA at different methanol concentrations. To ease the effect of cathode water flooding and ensure the stability of the fuel cell, the polarization tests were carried out at constant surrounding temperature of 333 K in the thermostatic container. CP-MEA achieved its peak power density of 38.9 mW cm^{-2} at 2 M methanol concentration, while SSFF-MEA achieved its peak power density of 42.4 mW cm^{-2} at 3 M methanol concentration. Table 2 summaries the peak power densities and open-circuit voltage (OCV) of CP-MEA and SSFF-MEA at different methanol concentrations. At low methanol concentrations of 1 M and 2 M where methanol crossover is small, the difference in peak power density and OCV was not obvious. After that, the difference increased greatly with methanol concentration, especially at 5 M methanol concentration where the peak power density of SSFF-MEA exhibited 50% higher than that of CP-MEA and the OCV was 30% higher correspondingly. It can be seen that SSFF-MEA enables the cell operated at a higher methanol concentration and exhibits better performance than CP-MEA. This reveals that SSFF-MEA has a greatly reduced methanol crossover compared with CP-MEA.

Table 2
Peak power densities and open-circuit voltages of SSFF-MEA and CP-MEA with different methanol concentrations.

Methanol concentration (M)	SSFF-MEA		CP-MEA	
	Peak power density (mW cm^{-2})	Open-circuit voltage (V)	Peak power density (mW cm^{-2})	Open-circuit voltage (V)
1	34.13	0.74	31.40	0.69
2	39.98	0.71	38.99	0.63
3	42.41	0.69	37.06	0.59
4	39.78	0.68	32.16	0.54
5	35.71	0.66	24.05	0.50

To gain an insight understanding about effects of MEA structure on the cathode and anode electrode processes, the electrode potentials were measured separately in-situ with an Ag/AgCl reference electrode and shown in Fig. 5. Fig. 5(a) shows the cathode potentials of SSFF-MEA and CP-MEA at the methanol

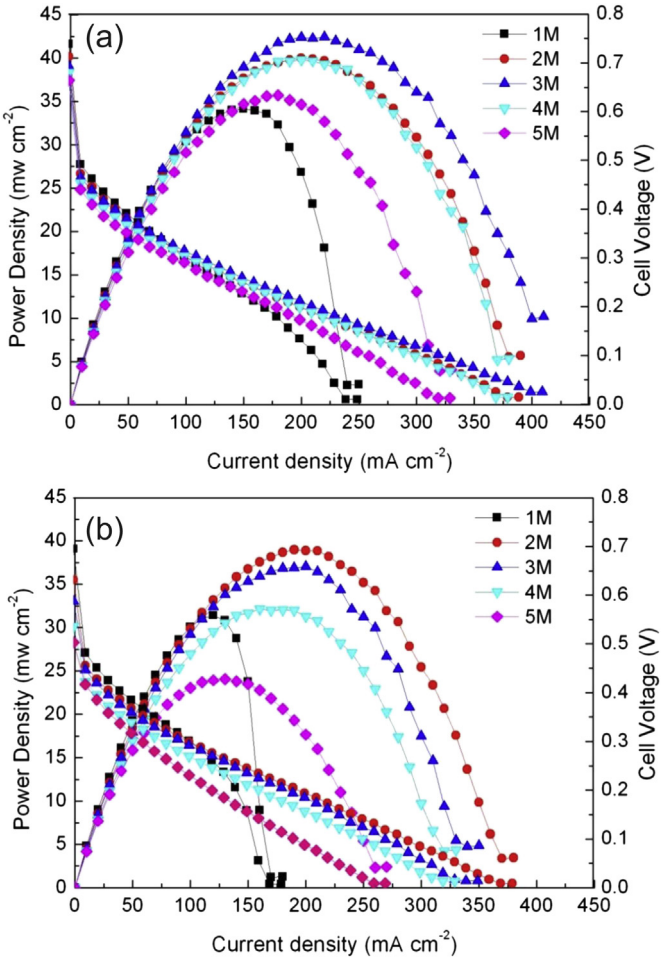

Fig. 4. Power density curves of CP-MEA (a) and SSFF-MEA (b) with different methanol concentrations at 333 K.

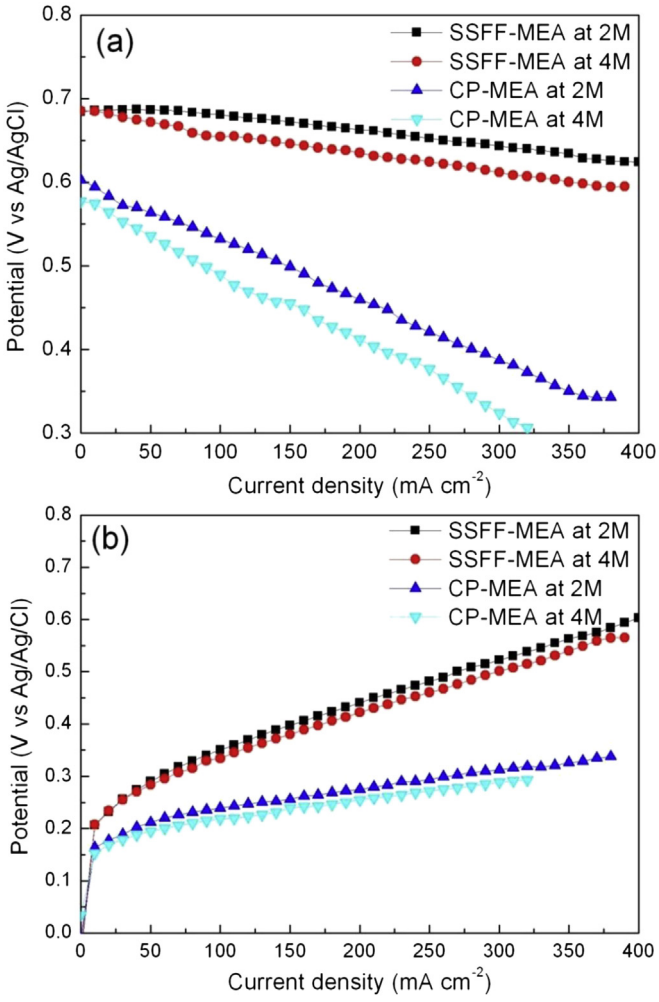

Fig. 5. Cathode (a) and anode (b) potentials of SSFF-MEA and CP-MEA with 2 M and 4 M methanol solutions.

concentrations of 2 M and 4 M. The cell voltage equals to the difference between the anode and cathode potentials, and a higher cathode potential or a lower anode potential means a smaller electrode polarization, which stands for a higher voltage and a better cell performance. During the discharging process, SSFF-MEA had a much higher cathode potential than CP-MEA, especially at 4 M methanol concentration. This result confirms that SSFF-MEA has a significantly reduced methanol crossover. The methanol crossover increased with the current density, which made the cathode potential of CP-MEA decline more rapidly than that of SSFF-MEA and made their differences in the electrode potentials enlarge further at high current density.

The decreased methanol crossover can be attributed to the even distribution of the package pressure over SSFF-MEA. At the cathode of a conventional MEA, the area contacting with the current collector has a much larger package pressure than that opening to air, and then methanol can transport more easily through the Nafion membrane at the latter area to cathode, leading to the increase of methanol crossover of the fabricated cell. SSFF-MEA uses SSFF as the cathode current collector and backing layer, which allows the cathode package pressure distribute uniformly over the MEA. Therefore, the methanol transportation through the whole Nafion membrane was almost equal and small, making the fabricated cell give a low methanol crossover. Moreover, the low porosity of the SSFF, which is 7.2% lower than CP, also decreases the methanol crossover at a certain extent.

An interesting result shown in Fig. 5(b) is that SSFF-MEA has a higher anode potential than CP-MEA, that is, the anode electrode process inside SSFF-MEA has a stronger polarization than that inside CP-MEA. This can be attributed to the temperature difference inside the two MEAs. Methanol transporting through Nafion membrane from anode to cathode is oxidized directly with oxygen:

$$CH_3OH + \frac{3}{2}O_2 \rightarrow CO_2 + 2H_2O \quad (1)$$

Although this reaction leads to a mixed potential and increases the cathode polarization, it also generates plenty of heat ($\Delta G = -698.2$ kJ mol^{-1}) that raises the inner temperature of MEA and thus decreases the activation polarization of the electrode process. For the cathode reaction of oxygen reduction, this decrease in polarization is smaller than the potential drop caused by methanol crossover, which makes the cathode polarization still increase with methanol crossover. But for the anode reaction of methanol oxidation that has a larger activation polarization, a larger methanol crossover can generate more heat that decreases the anode polarization. Consequently, the anode polarization decreases with methanol crossover. The previous results show that CP-MEA has a larger methanol crossover than SSFF-MEA. In this case, CP-MEA generates a higher inner temperature than SSFF-MEA, which reduces its anode polarization.

3.3. Performance tests at different operation temperatures

To explore the performance of the two MEAs at different surrounding temperature, the polarization tests at 298 K (room temperature) and 333 K with a methanol concentration of 2 M were performed, as shown in Fig. 6. The maximum power densities of SSFF-MEA and CP-MEA at 298 K are 20.5 mW cm^{-2} and 15.5 mW cm^{-2}, respectively. It could be found that the difference in performances of the two MEAs became much more obvious at 298 K than that at 333 K. At high temperature, water flooding inside the MEA was not seriously and had a little influence on oxygen transportation. But at room temperature, water could

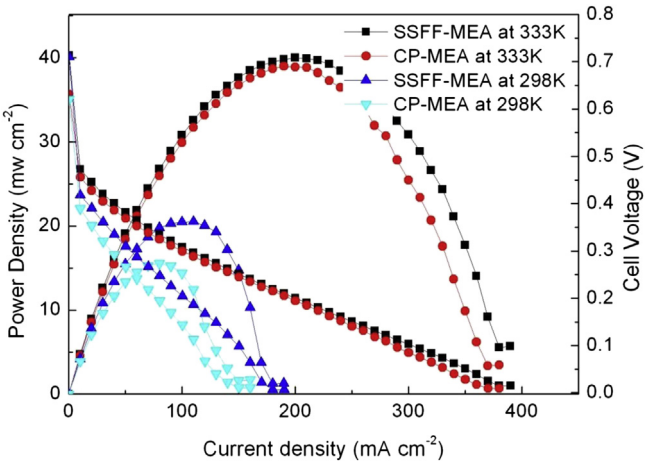

Fig. 6. Power density curves of SSFF-MEA and CP-MEA with 2 M methanol solution at 298 K and 333 K.

easily accumulate inside the cathode gas diffusion layer, which hindered oxygen transportation in great extent. In this case, a much better performance of SSFF-MEA at room temperature may mean that SSFF-MEA suffers less from water flooding problem than CP-MEA.

The reason that SSFF-MEA gives a better water management than CP-MEA may arise from the following three aspects. Firstly, water is one of the oxidation reaction productions of methanol crossover, and CP-MEA has a higher methanol crossover than SSFF-MEA, which made more water produced in its cathode catalyst layer and thus increased the water flooding problem. Secondly, CP-MEA has its cathode catalyst layer exposed directly to air with a ratio of 29.2% (calculating by multiplying the CP porosity 73% with the current collector open ratio 40%), while SSFF-MEA has the same exposing area ratio of 65.8% as the SSFF porosity. This indicates that the structure of SSFF-MEA enlarges open area for water removal, which is beneficial to avoid water flooding at cathode and also improves oxygen transportation. Thirdly, the results in Fig. 3 show that SSFF has a more hydrophilic surface than CP does, and in this case, water is more capable of being dragged out of the catalyst layer in SSFF-MEA, which can lower water flooding inside gas diffusion electrode and enhance oxygen transportation. Therefore, SSFF-MEA exhibited better oxygen transportation than CP-MEA when discharging at room temperature.

To evaluate the stability and the fuel utilization ratio of SSFF-MEA, the fabricated cell was discharged under a constant current density of 100 mA cm^{-2}. Fig. 7(a) and (b) shows the test results achieved with 6.35 wt.% 2 mL methanol solutions at surrounding temperatures of 333 K and 298 K. During the discharging in 333 K, the difference in output voltages of the two MEAs was not obvious as high temperature made liquid water can hardly accumulate at cathode. As shown in Fig. 7(b), the cathode and anode potentials of SSFF-MEA are about 0.2 V higher than those of CP-MEA due to the reduced methanol crossover. And with the higher output voltage, SSFF-MEA lasts 20 min longer than CP-MEA. It should be noticed that at the end of the discharging test, the anode potential increased sharply due to methanol depletion, but the cathode potential did nearly not changed, which means that the cathode polarization was not influenced by the methanol consumption of anode reaction. Measured by gas chromatograph, the methanol solution in the reservoirs was decreased to 1.15 wt.% 1 mL for SSFF-MEA and 1.48 wt.% 0.8 mL for CP-MEA. It can be found that with the reduced methanol crossover and the lower overpotential, SSFF-MEA can consume methanol solution more thoroughly, so

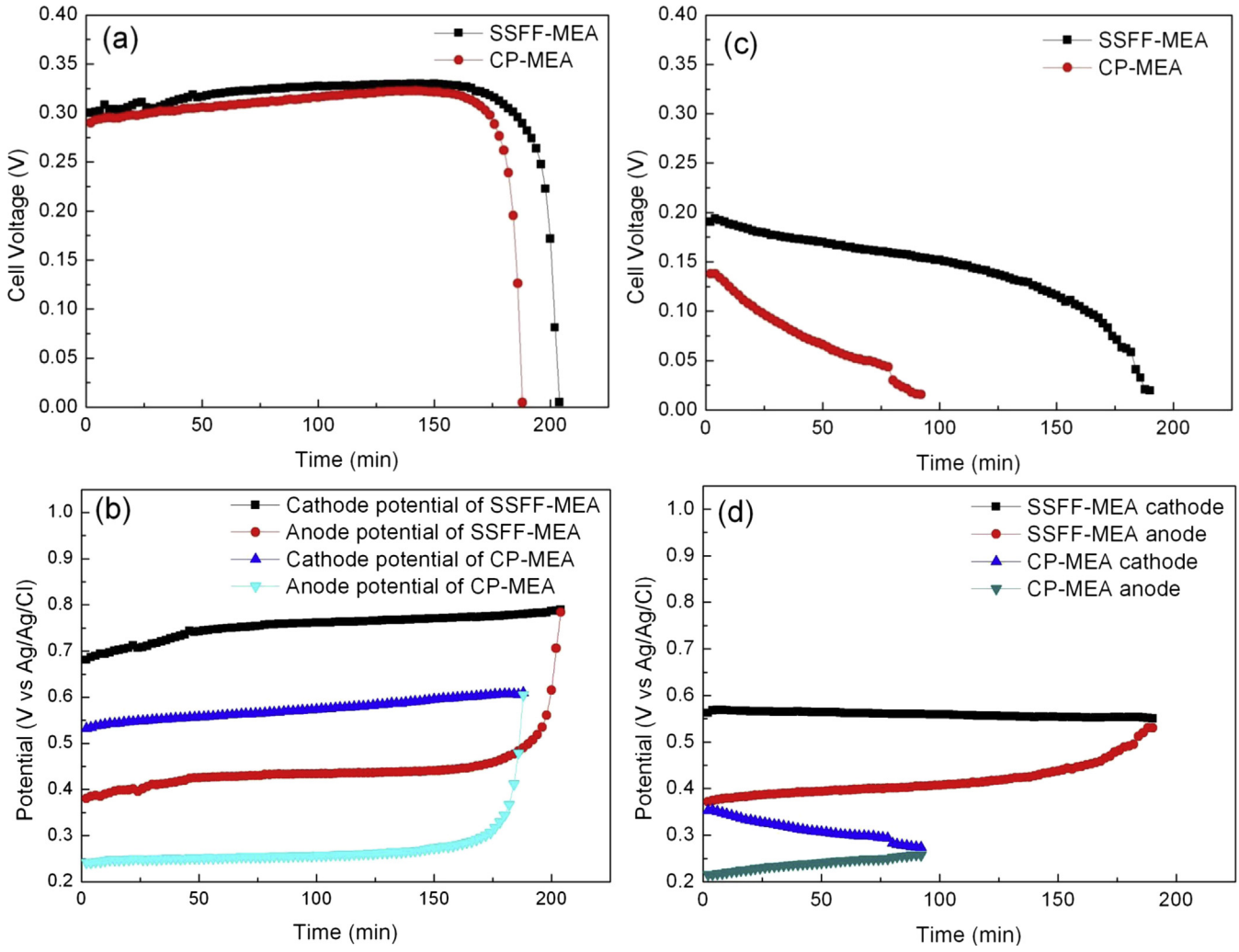

Fig. 7. Cell voltages (a, c) and electrode potentials (b, d) of SSFF-MEA and CP-MEA discharging under 100 mA cm^{-2} at 333 K (a, b) and 298 K (c, d).

the final concentration was lower. Comparing with the CP cathode with stainless steel current collector, the lower porosity and temperature of the SSFF cathode also reduced the evaporation in high temperature, so a difference in the final solution volume was detected.

Energy efficiency ζ and Faradic conversion efficiency η were calculated with the following equations [32],

$$\zeta = \frac{\int_0^t I u_t \mathrm{d}t}{\left(V_0 c_0 - V_f c_f\right)\Delta G} \times 100\% \quad (2)$$

$$\eta = \frac{It}{6F\left(V_0 c_0 - V_f c_f\right)} \times 100\% \quad (3)$$

where I is the discharge current; t the time of the discharge process; u_t the discharge voltage; V_0 the volume of the initial solution; c_0 the concentration of the initial solution; V_f the volume of the final solution; c_f the concentration of the final solution; ΔG the change of the Gibbs free energy of the oxidation reaction of methanol; F the Faradic constant. Faradic efficiency is here defined as a ratio of actual discharge capacity versus theoretical capacity of fuel, and actually, it equals to the fuel utility. Energy efficiency is a percentage of electric energy generated in a fuel cell versus the theoretical chemical energy of the total fuel consumed. Table 3 shows the calculated values of energy and faradic efficiencies at 333 K. The results show that energy efficiencies of SSFF-MEA and CP-MEA were 37.3% and 33.7%, respectively. Faradic efficiencies of SSFF-MEA and CP-MEA were 61.3% and 55.6%, respectively. It can be found that as a result of the reduced methanol crossover, SSFF-MEA has higher energy efficiency and better Faradic efficiency than CP-MEA.

The advantages of SSFF-MEA were more obviously when discharging at 298 K, as shown in Fig. 7(c) and (d). The output voltage of CP-MEA dropped sharply, while the output voltage of SSFF-MEA exhibited a slower decrease. The anode potentials of the two MEAs varied nearly in the same way, reflecting as a slight increase with the discharging time due to the methanol consumption. Hence, the difference in output voltages mainly arises from the cathode polarization behaviors, as shown in Fig. 7(d) where SSFF-MEA gives a higher and more stable potential than CP-MEA. The advantages of SSFF-MEA are mainly due to its novel cathode structure, which eliminates cathode current collector and has more passages for the mass transportation. In addition, the novel cathode structure allows water to distribute on its surface in shapes of small droplets, as

Table 3
Faradic and energy efficiencies of SSFF-MEA and CP-MEA calculated with the initial methanol solution of 6.35 wt.% 2 ml.

		SSFF-MEA	CP-MEA
333 K	Final volume (ml)	1.00	0.80
	Final concentration (wt. %)	1.15	1.48
	Faradic efficiency (%)	61.30	55.62
	Energy efficiency (%)	37.30	33.65
298 K	Final volume (ml)	1.80	1.80
	Final concentration (wt. %)	3.25	4.87
	Faradic efficiency (%)	93.88	77.50
	Energy efficiency (%)	26.83	11.67

shown in Fig. 8(a) where small droplets are easily dropped off by gravity. While the droplets on the conventional cathode was much bigger and could easily submerge the air-transportation hole of the current collector, as shown in Fig. 8(b) where lots of holes in the conventional cathode current collector were submerged. In this case, SSFF-MEA has more sufficient oxygen feeding in the situation of water flooding.

At 298 K, the 100 mA discharging tests of SSFF-MEA and CP-MEA lasted for about 190 min and 90 min, respectively. Consumed from the initial concentration of 6.35 wt.% 2 mL, the final methanol solution was 3.25 wt.% 1.8 mL for SSFF-MEA and 4.87 wt.% 1.8 mL for CP-MEA. Energy and Faradic efficiencies were obtained by Equations (2) and (3) and listed in Table 3. Energy efficiencies were 26.8% for SSFF-MEA and 11.7% for CP-MEA. Faradic efficiencies were 93.9% and 77.5% for SSFF-MEA and CP-MEA, respectively. It can be seen that the reduced methanol crossover and the improved water management of SSFF-MEA made its energy efficiency and Faradic efficiency increase significantly, especially energy efficiency, which was more than doubled when compared with CP-MEA at room temperature.

3.4. EIS measurements

To further elaborate the effect of the novel structure on the MEA performance, electrochemical impedance spectra (EIS) measurements at the discharging current density of 20 mA cm^{-2} and 80 mA cm^{-2} with 2.0 M methanol solution were carried out at 333 K, and the results were shown in Fig. 9. It was pointed out that the right intercept with the real coordinate axis on Nyquist plot (low frequency data) is related to the charge transfer resistance (CTR) of the electrode reaction. A high CTR indicates a large reaction resistance and a strong polarization of the electrode process. The inductive loop in the lowest frequency range arises from the absorption/desorption of CO as a result of the methanol oxidation reaction [33,34].

Because of the oxidation of the methanol transporting from the anode through Nafion membrane, the cathode impedance can also appear as an inductive loop. However, the novel cathode did not show the inductive loop in its lowest frequency, while the conventional one did. This indicates clearly that there was less methanol oxidation reaction occurring inside the novel cathode, that is, it confirms again that SSFF-MEA has a less methanol crossover than CP-MEA. The novel cathode also exhibited a much smaller CTR than did the conventional one, indicating a smaller reaction resistance and a weak cathode polarization, which was consistent with the cathode polarization curves shown in Fig. 4.

As for the anode impedance, SSFF-MEA presented a larger CTR value than CP-MEA, especially at the discharging current density of 80 mA cm^{-2}. This result proves the rationality of our explanations about the variation of inner temperature with methanol crossover, that is, higher methanol crossover lead to a higher inner temperature and decreased the activation polarization and the CTR of anode process.

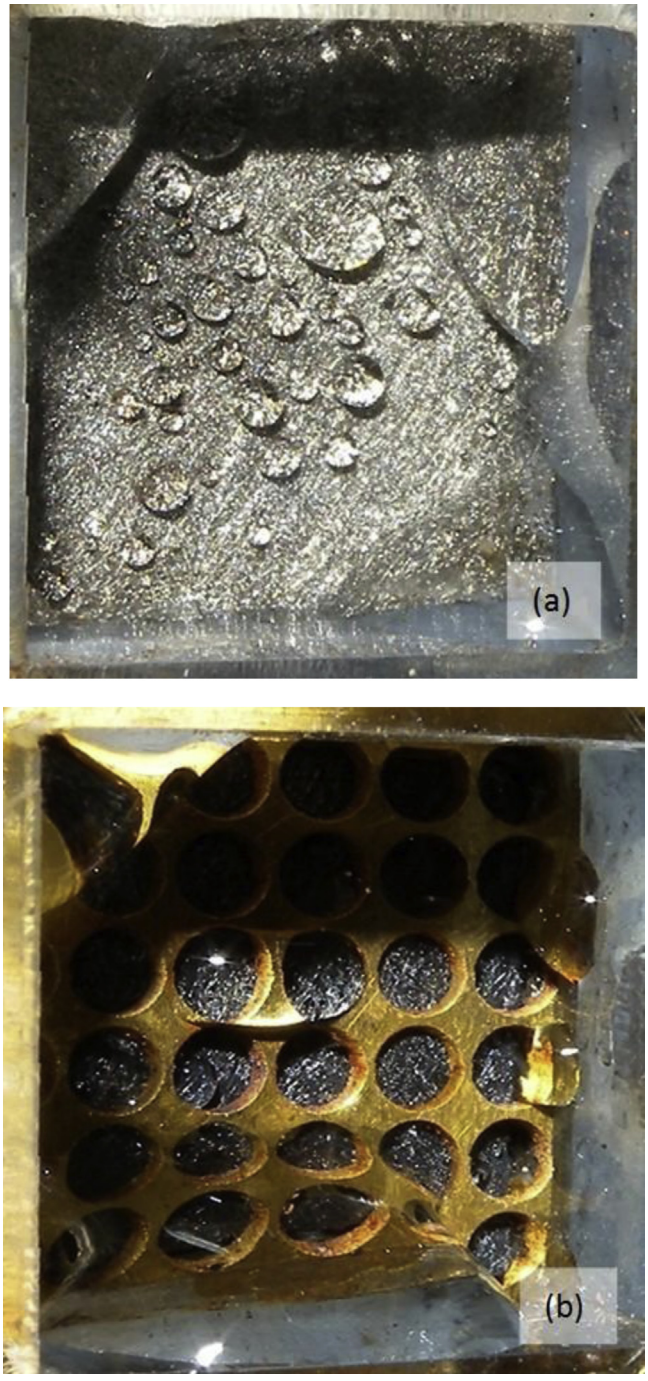

Fig. 8. Water flooding of the novel (a) and conventional (b) cathodes after discharging under 100 mA cm^{-2} for a long period at 298 K.

The impedance spectra of full cell reveals that SSFF-MEA has a slightly increased inner resistance compared with that of CP-MEA, expressed as a more left intercept with the real coordinate axis in the high frequency range. This also proves that SSFF can maintain good interfacial contact in cell configuration. If IR corrections are made to the measured voltages [24], SSFF-MEA can give a much better performance than CP-MEA. In the low frequency range, the impedance spectra of SSFF-MEA showed small CTRs than CP-MEA,

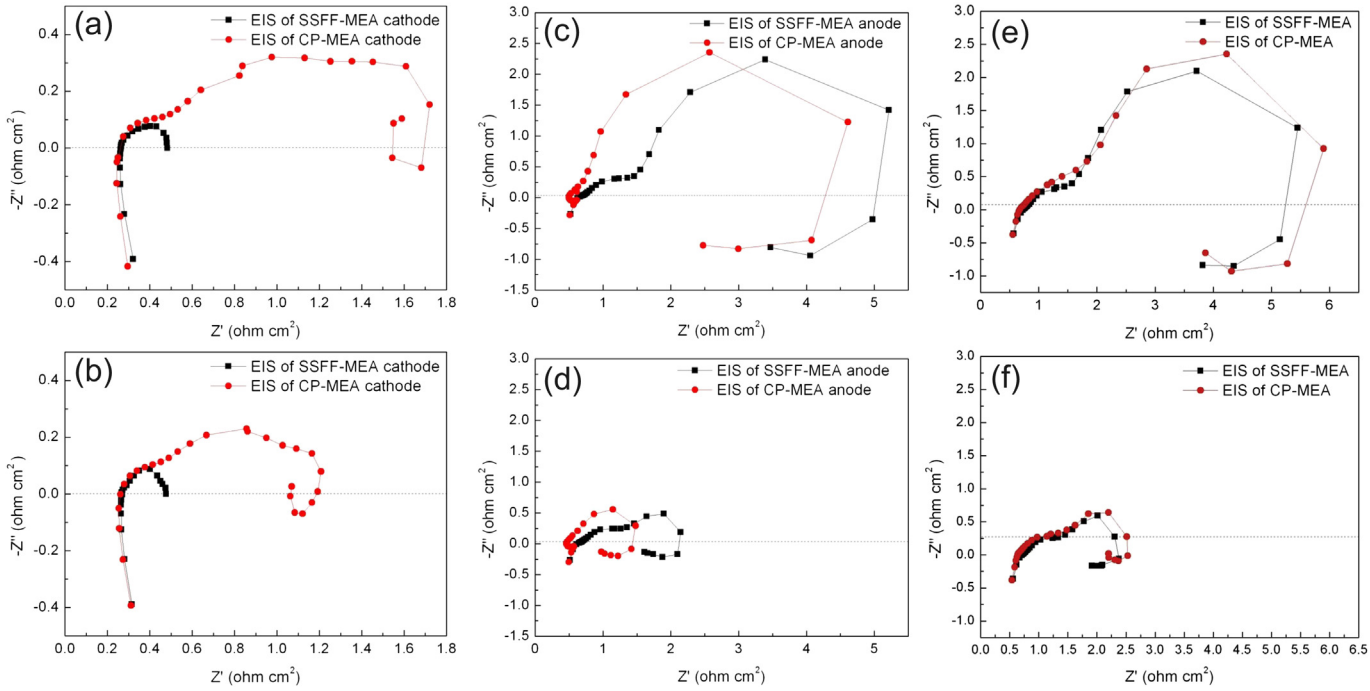

Fig. 9. EIS spectra of the cathode (a, b), anode (c, d), and full cell (e, f) of SSFF-MEA and CP-MEA discharging under 20 mA cm^{-2} (a, c, e) and 80 mA cm^{-2} (b, d, f) with 2 M methanol solution.

confirming that SSFF-MEA has small electrode polarizations and better performance.

4. Conclusions

With the application of stainless steel fiber felt (SSFF) as cathode backing layer and current collector, the structure of a passive DMFC is more integrated and supplies another resolution to optimize cathode current collector open ratio. The mechanical strength of the adopted SSFF is strong enough to maintain the required assembly pressure to ensure the good interfacial contact when fabricating a cell. Inside the novel structure, methanol crossover was reduced dramatically due to an even package pressure distribution and a lower porosity. The electrochemical results of half-cell test reveal that the reduced methanol crossover can make the cathode potential increased more than 200 mV, indicating a greatly reduced cathode polarization, although it also leads to a slightly increased anode polarization. A constant-current-density discharging test at 333 K shows that the reduced methanol crossover can make the energy and Faradic efficiencies increased from 33.6% to 37.1% and 55.6% to 61.3%, respectively. In addition, the novel structure also gives a better water management at room temperature, which can make the energy and Faradic efficiencies increased from 11.7% to 26.8% and 77.5% to 93.9%, respectively. EIS measurement also confirms that the novel structure has less methanol crossover and smaller cathode polarization. In conclusion, the MEA fabricated with SSFF gives better performance than a conventional one, which results from both the new material and the novel configuration.

Acknowledgments

This work was supported by the National Natural Science Funds of China (No. 60806037, 61076105 and 61176109) and the Fundamental Research Funds for the Central Universities (Grant No. HIT. NSRIF. 2010075).

References

[1] S.K. Kamarudin, F. Achmad, W.R.W. Daud, Int. J. Hydrogen Energy 34 (2009) 6902–6916.
[2] T.S. Zhao, C. Xu, R. Chen, W.W. Yang, Prog. Energy Combust. Sci. 35 (2009) 275–292.
[3] T.S. Zhao, C. Xu, R. Chen, W.W. Yang, J. Power Sources 191 (2009) 185–202.
[4] F. Zenith, U. Krewer, Energy Environ. Sci. 4 (2011) 519–527.
[5] H. Ahmad, S.K. Kamarudin, U.A. Hasran, W.R.W. Daud, Int. J. Hydrogen Energy 35 (2010) 2160–2175.
[6] L. Li, F.J. Shang, L. Wang, S.P. Pei, Y.M. Zhang, Energy Environ. Sci. 3 (2010) 114–116.
[7] X.L. Zhang, Y.F. Zhang, N. Li, X.W. Liu, L.M. Chang, J. Power Sources 216 (2012) 525–529.
[8] S. Mohanapriya, S.D. Bhat, A.K. Sahu, S. Pitchumani, P. Sridhara, A.K. Shukl, Energy Environ. Sci. 2 (2009) 1210–1216.
[9] M.A. Abdelkareem, N. Morohashi, N. Nakagawa, J. Power Sources 172 (2007) 659–665.
[10] Y.H. Chan, T.S. Zhao, R. Chen, C. Xu, J. Power Sources 176 (2008) 183–190.
[11] C.E. Shaffer, C.Y. Wang, J. Power Sources 195 (2010) 4185–4195.
[12] H.K. Kim, J. Power Sources 162 (2006) 1232–1235.
[13] L.G. Feng, J. Zhang, W.W. Cai, L. Liang, W. Xing, C.P. Liu, J. Power Sources 196 (2011) 2750–2753.
[14] Q.X. Wu, T.S. Zhao, R. Chen, W.W. Yang, Int. J. Hydrogen Energy 35 (2010) 10547–10555.
[15] T.T. Wang, C.S. Lin, F. Ye, Y. Fang, J.J. Li, X.D. Wang, Electrochem. Commun. 10 (2008) 1261–1263.
[16] A. Blum, T. Duvdevani, M. Philosoph, N. Rudoy, E. Peled, J. Power Sources 117 (2003) 22–25.
[17] H.K. Kim, J.M. Oh, J.H. Kim, H. Chang, J. Power Sources 162 (2006) 497–501.
[18] J.Y. Cao, M. Chen, J. Chen, S.J. Wang, Z.Q. Zou, Z.L. Li, D.L. Akins, H. Yang, Int. J. Hydrogen Energy 35 (2010) 4622–4629.
[19] P.Y. Yi, L.F. Peng, X.M. Lai, M.T. Li, J. Ni, Int. J. Hydrogen Energy 37 (2012) 11334–11344.
[20] J.G. Liu, G.Q. Sun, F.L. Zhao, G.X. Wang, G. Zhao, L.K. Chen, B.L. Yi, Q. Xin, J. Power Sources 133 (2004) 175–180.
[21] R. Chen, T.S. Zhao, Electrochem. Commun. 9 (2007) 718–724.
[22] W.M. Yang, S.K. Chou, C. Shu, J. Power Sources 164 (2007) 549–554.
[23] S.H. Yang, C.Y. Chen, W.J. Wang, J. Power Sources 195 (2010) 2319–2330.
[24] P. Piela, T.E. Springer, J. Davey, P. Zelenay, J. Phys. Chem. C 111 (2007) 6512–6523.
[25] Z. Liu, J.S. Wainright, W. Haung, R.F. Sacinell, Electrochim. Acta 49 (2004) 923–935.

[26] S. Eccarius, T. Manurung, C. Ziegler, J. Electrochem. Soc. 154 (2007) B852–B864.
[27] J. Zhang, G.P. Yin, Y.Y. Shao, Z.B. Wang, Q.Z. Lai, Rare Met. Mater. Eng. 37 (2008) 476–479.
[28] A. Marmur, Soft Matter 2 (2006) 12–17.
[29] Wei Yuan, Yong Tang, Xiaojun Yang, Zhenping Wan, Appl. Energy 94 (2012) 309–329.
[30] Andrzej Gajewski, Int. J. Heat Mass Transf. 51 (2008) 4628–4636.
[31] Yong Tang, Wei Yuan, Minqiang Pan, Zhenping Wan, Int. J. Hydrogen Energy 35 (2010) 9661–9677.
[32] Deryn Chu, Rongzhong Jiang, Electrochim. Acta 51 (2006) 5829–5835.
[33] J.T. Mueller, P.M. Urban, J. Power Sources 75 (1998) 139–143.
[34] J.T. Mueller, P.M. Urban, W.F. Holderich, J. Power Sources 84 (1999) 157–160.